ICAST2014 #020

A pair of piezo-based rotating inertial actuators for active structural acoustic control of rotating machinery

Guoying Zhao[1], Neven Alujevic[1], Bruno Depraetere[2], Gregory Pinte[2], Jan Swevers[1], Paul Sas[1]

[1] KU Leuven, Department of Mechanical Engineering, Heverlee, Belgium
[2] Flanders Mechatronics Technology Centre, Heverlee, Belgium

Abstract

In this paper, two Piezo-Based Rotating Inertial Actuators (PBRIAs) are considered for the suppression of the structure-borne noise radiated from rotating machinery. As add-on devices, they can be directly mounted on a rotational shaft, in order to intervene as early as possible in the transfer path between disturbance and the noise radiators. A MIMO form of the modified FxLMS control algorithm is employed to generate the appropriate actuation signals, relying on a linear interpolation scheme to approximate the nonlinear secondary plants. The proposed active vibration control approach is tested on an experimental test bed comprising a rotating shaft mounted in a frame to which a noise-radiating plate is attached. The disturbance force is introduced by an electrodynamic shaker. The experimental results show that when the shaft rotates below 180 rpm, more than a 7 dB reduction can be achieved in terms of plate vibrations, along with a reduction in the same order of magnitude in terms of noise radiation.

1. INTRODUCTION

Noise radiation from structural housing in rotating machinery is a common problem in many industrial applications such as gearboxes, compressors, electric motors etc. In these cases, vibrations of rotating elements, which are transmitted though the bearings to the noise radiating surfaces such as the machine frame, are often the major noise source. In order to reduce the received noise level, techniques such as sound absorption based on insulation, including encapsulation, can be used to interrupt the airborne sound transmission from the machine to the environment. These passive sound control techniques would typically be used to deal with noise at higher frequencies. At lower frequencies, where the acoustic wavelength is much larger than the maximum permissible thickness of the insulation layers, active noise control strategies can be considered instead [1-4]. These however become more complicated and more expensive, or alternatively less efficient, if the size of the enclosure where the sound is controlled [3] is comparatively large. Lots of error sensors and control actuators are necessary for good control performance, and in fact the total length of the wiring to connect peripheral units to the centralised controller can become a limitation [4]. In such situations it could be preferred to directly reduce the vibro-acoustic response of the noise radiating surfaces. This can be done by applying control forces on the surfaces [5, 6, 11-17] or isolating the transmission force to the surfaces [18-25]. In case forces are applied directly to the noise radiation surfaces, passive tuned mass dampers [7-10], inertial shakers [11-13],

reactive actuators [14] or piezoelectric patches [15-17] are often employed to produce the control forces. However, this approach may become cumbersome and expensive for large and complex systems which have many radiating surfaces.

On the other hand, in the active vibration isolation approach it is attempted to block the transmitted vibrations in the structural transfer paths before they reach the noise radiating surfaces. This may yield a control system that is less complex in case there are concentrated bottlenecks in the vibration transmission paths. With rotating machinery such concentrations typically occur in bearings that support revolving shafts. Several studies based on this approach have been published recently. Rebbechi et al. [19] proposed to integrate two pairs of magnetostrictive actuators into a double row bearing, which is mounted on the input shaft next to the input pinion, with the aim of actively isolating the vibration transmitted from the shaft to the housing. A reduction of 20-28 dB can be obtained in the housing vibration at the fundamental gear mesh frequency. Pinte et al. and Stallaert et al. [20-21] adopted a similar approach, but used two piezoelectric actuators instead, which are perpendicularly mounted onto one of the support bearing locations in order to limit the force transmitted from the shaft to the housing. Chen and Brennan [22] presented an inertial actuator control concept, where three magnetostrictive inertial shakers are positioned tangentially at 120° intervals on the gear body, in order to suppress the gear vibrations at the source. The above mentioned actuation concepts for the suppression of gearbox housing vibrations are theoretically compared by Guan et al. [23]. In this theoretical study, the actuation effort, control robustness and implementation costs are taken into account as the comparison criteria for four different actuation concepts. The shaft transverse vibration active control approach appeared to be the best compromise regarding the required amplitude of the control force below 500 Hz and fairly reasonable other control parameters in the higher frequency range. Some experimental validation concerning this theoretical study can be found in [24-25].

In this study, an axisymmetric piezo-based rotational inertial actuator, which can be installed directly on the rotating shaft as an add-on device, is proposed and studied experimentally. The benefit of this add-on approach is that the machine stiffness is not affected as is the case with for example active bearings. Another advantage is the relative ease of implementation in a practical setting as no major structural modification is required. Furthermore, the active element is not in a critical path of the machine such that a possible failure of the piezoelectric element does not necessarily affect the functionality of the machine.

One of the aims of this paper is to investigate whether or not it is feasible to suppress tonal structural borne noise/vibration by attaching PBRIAs directly onto a rotating shaft. The control strategy is based on the modified filtered reference least mean squares (FxLMS) algorithm [26]-[27]. Such an algorithm has been adapted in this study for the use on rotating machine applications by utilising an interpolation scheme for time varying secondary plants. The design of the PBRIA is briefly covered in Section 2, together with the experimental test bed used to evaluate its performance. The implementation of the modified FxLMS control algorithm is discussed next, in Section 3, followed by a presentation of the achieved results in Sections 4.

2. DESIGN OF PIEZO-BASED ROTATING INERTIAL ACTUATOR

Figure 1 shows the developed prototype of the piezo-based rotating inertial actuator. The idea behind the design of the PBRIA is to use a piezoelectric actuator to introduce a force between a rotating element (e.g. the shaft) and a ring-shaped mass rotating together with the shaft. By accelerating the ring-shaped mass, compensating forces can be generated on the shaft. The Piezomechanik HPSt 150/20 piezoelectric stack actuator is used. Although the piezoelectric actuator has a sufficient stroke to compensate the disturbances on the test bed, it is acknowledged that in stiff industrial applications, where excitation forces are larger, longer piezoelectric actuators with larger sections should be used to generate the required strokes. The piezoelectric actuator is preloaded by the flexures on the other side, such that it is capable of

applying bi-directional (push/pull) forces. In order to avoid bending of the piezoelectric stack actuator, four Z shaped springs are foreseen at each corner, with the actuator centrally located. For the Z shaped spring, the vertical links are much shorter and, more importantly, thicker than the horizontal links such that a high rotational stiffness and a low horizontal stiffness are realized.

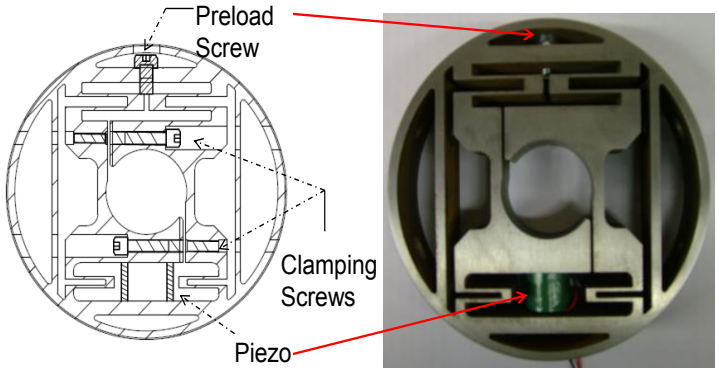

Figure 1. The developed piezo-based rotating inertial shaker.

A representative set-up for rotating machinery is constructed in order to demonstrate the feasibility of the proposed active vibration control approach, which is shown in Figure 2. In this test bed, a motor drives a shaft, which is supported in a frame by a cylindrical bearing at one side and a double angular contact ball bearing at the other side. This latter bearing is mounted in a ring-shaped module in which two piezoelectric sensors are installed to measure the transmitted forces between the shaft and the frame. Close to this bearing, two PBRIAs are perpendicularly installed on the shaft such that control forces can be generated in all directions. In order to transmit control signals from a non-rotating control source, a slip ring is equipped and mounted on the shaft close to the PBRIAs to provide electrical connections to the non-rotating controller.

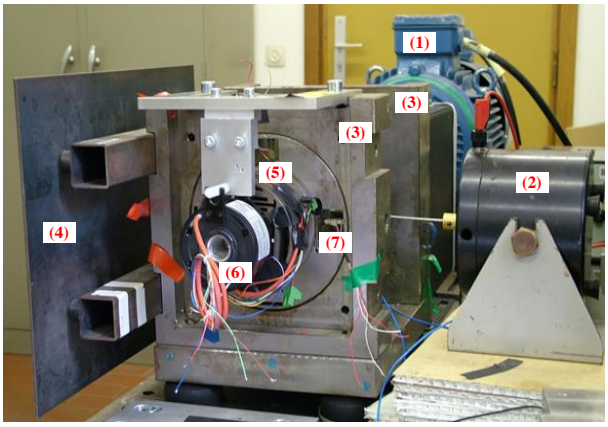

Figure 2. The experimental set-up of the test bed: (1) Motor; (2) Disturbance shaker; (3) Frame; (4) Noise radiating plate; (5) PBRIAs; (6) Slip ring; (7) Force sensor.

A number of sensors are installed on and around the test bed to demonstrate the performance of the proposed control approach. The layout of the sensor configuration is shown in Figure 3, where two accelerometers are used to measure the structural vibrations, one microphone is used to register the noise level in front of the plate at a distance of approximately 30 cm and one force gauge placed between the bearing close to the PBRIA and the frame is used to record the transmission force. For the accelerometers, one of them is placed on the frame measuring vibrations in x and y axes, while the other one is mounted in

the middle of the plate measuring only vibrations in *x* axis. The *x* and *y* axes represent the directions that are parallel and perpendicular to the disturbance line of action, as indicated in Figure 3. Hereafter, *x* direction refers to as the horizontal direction and *y* direction refers to as the vertical direction. The frame vibrations in the *y* axis (the vertical frame acceleration) and plate vibrations in the *x* axis (the horizontal plate acceleration) are chosen as the error signals for the active controller in the experiments of this study.

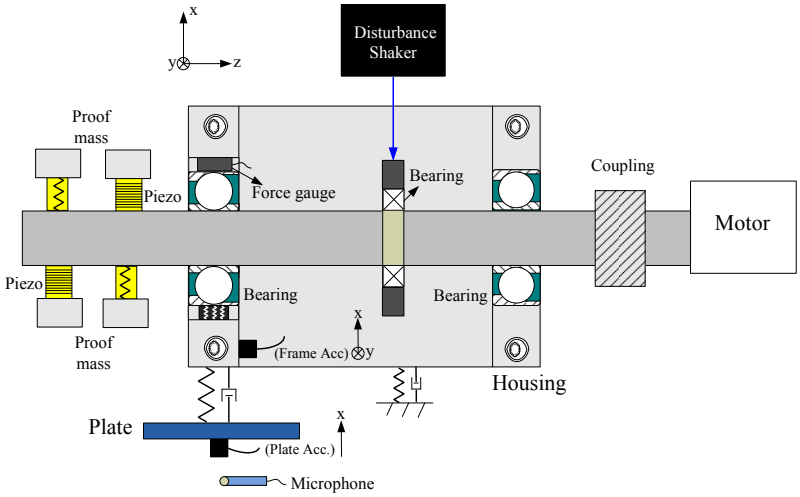

Figure 3. A cross-sectional view of the experimental set-up with all measurements

3. MODIFIED FxLMS ADAPTIVE CONTROLLER

In this section, the modified FxLMS control algorithm [26]-[27] is briefly reviewed. Its control scheme is shown in Figure 4, where $\bar{d}(k)$ is the estimate of the disturbance $d(k)$ used to derive the virtual error signal $e_m(k)$ for updating the control filter coefficients; $e(k)$ is the physical error signal measured by the error sensor; $\bar{S}(q)$ is the estimate of the secondary plant; $x(k)$ represents the reference signal; the coefficients of $\bar{W}(k)$ for generating the control signal $u(k)$ are copied from the adaptive filter $W(k)$ at the bottom of Figure 4.

Applying the gradient descent method to the adaptive filter in the lower loop of Figure 4 yields the adaptive scheme for $w_i(k)$:

$$w_i(k+1) = \beta w_i(k) + \mu r(k) e_m(k), i \in [0, L-1] \tag{1}$$

where $r(k)$ is the filtered reference signal calculated as the convolution of the reference signal and the model of the secondary plant, μ is the convergence coefficient, β is the power constraint with $0 < \beta \le 1$. Generally, the parameter μ should be as large as possible without compromising the stability of the system. A suitable value of control effort constrain β should be introduced to prevent unconstrained weight overflow and limit the output power to avoid nonlinear distortion [2]. If the parameter β is set to other value than 1, the modified FxLMS algorithm becomes the leaky modified FxLMS algorithm. Note that Eq. (1) is a direct form of instantaneous steepest descent algorithm, which can be derived by analogy

with the LMS algorithm. As such, the convergence speed of the modified FxLMS is reported to be comparable to that of the LMS algorithm [26]-[27].

Depending on the availability of the reference signal, the modified FxLMS algorithm can be used to control both broadband and narrowband disturbances. Considering the rotating machinery application, this study focuses on suppressing tonal disturbances and thereby the periodic modified FxLMS algorithm is implemented and a sinusoidal signal of the same frequency of the disturbance is used as the reference signal. If the aim is to suppress multiple tones at the fundamental frequency and several harmonics, the reference signal can be composed by a rectangular wave with a period equal to the inverse of the fundamental frequency of the disturbance or simply the sum of all the considered sinusoids [28]. Since two PBRIAs are used in the experiments, the MIMO form of the modified FxLMS algorithm is investigated. Here, the controlled plants are constructed between the driving signals to the two PBRIAs and the outputs of the two accelerometers measuring the horizontal plate vibrations and the vertical frame vibrations. Although the main focus of this study is on suppressing the noise radiation from the plate, only one accelerometer placed on the plate is in principle enough for the control purpose. The other error sensor is chosen so that the test bed is not seriously influenced in the vertical direction due to the control action. As mentioned earlier, the chosen error sensors are mounted on the fixed parts of the test bed whereas the piezoelectric actuators are rotating together with the shaft. This means that the constructed secondary plants are continually changing with respect to the shaft rotational position, which in other words indicates the secondary plants are time varying.

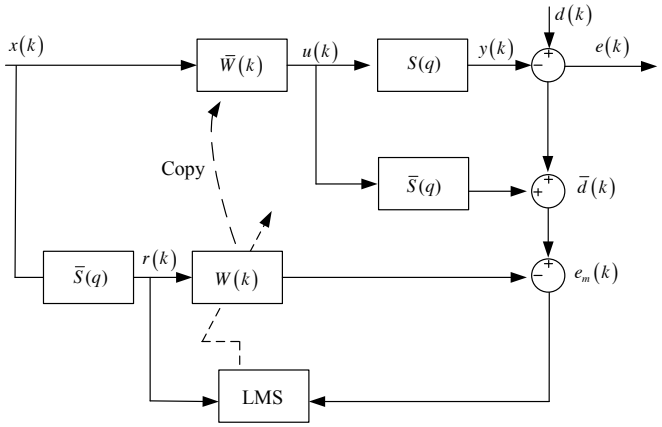

Figure 4. The block diagram of the modified FxLMS algorithm

A linear interpolation method is proposed to estimate the time varying secondary plants. The idea is to measure the secondary plants offline at several points in one revolution and estimate the rest by linearly interpolating between two adjacent known plants (the seed plants). As the secondary plants are modelled by FIR filters, the interpolation can be made directly on the coefficients of the FIR filters. If otherwise IIR (infinite impulse response) filters are used, the interpolation would best be implemented on the outputs of the IIR filters.

Finally, the flowchart of the employed MIMO form periodic modified FxLMS algorithm is depicted in Figure 5, where the various symbols have the following meanings: $x(k)$ again represents the reference signal which is presumed to be a sinewave and after undergoing a 90° phase shift, giving the other reference signal $x'(k)$; $W_1(q)$ and $W_2(q)$ are the two adaptive FIR filters, each of them is composed by two filter coefficients $w_{i,j}(q)$, $i, j \in [1,2]$, in addition, three other pairs of the copies from them are used; $y_1(n)$ and $y_2(n)$ are the driving signals for the two PBRIAs; $e_1(n)$ and $e_2(n)$ are the error signals

measured by the error sensors; $e_{v1}(n)$ and $e_{v2}(n)$ are the virtual error signals for updating the control filter coefficients; $y_{d1}(n)$ and $y_{d2}(n)$ are the disturbance sources measured by the error sensors; $[S_{11}(q)]_\theta$ and $[S_{21}(q)]_\theta$ are the secondary paths from $y_1(n)$ to the two error sensors at θ degrees; $[S_{12}(q)]_\theta$ and $[S_{22}(q)]_\theta$ are the secondary paths from $y_2(n)$ to the two error sensors; $\left[\overline{S_{i,j}}(q)\right]_\theta$ is the estimate of the secondary plant for $\left[S_{i,j}(q)\right]_\theta$, $i, j \in [1,2]$.

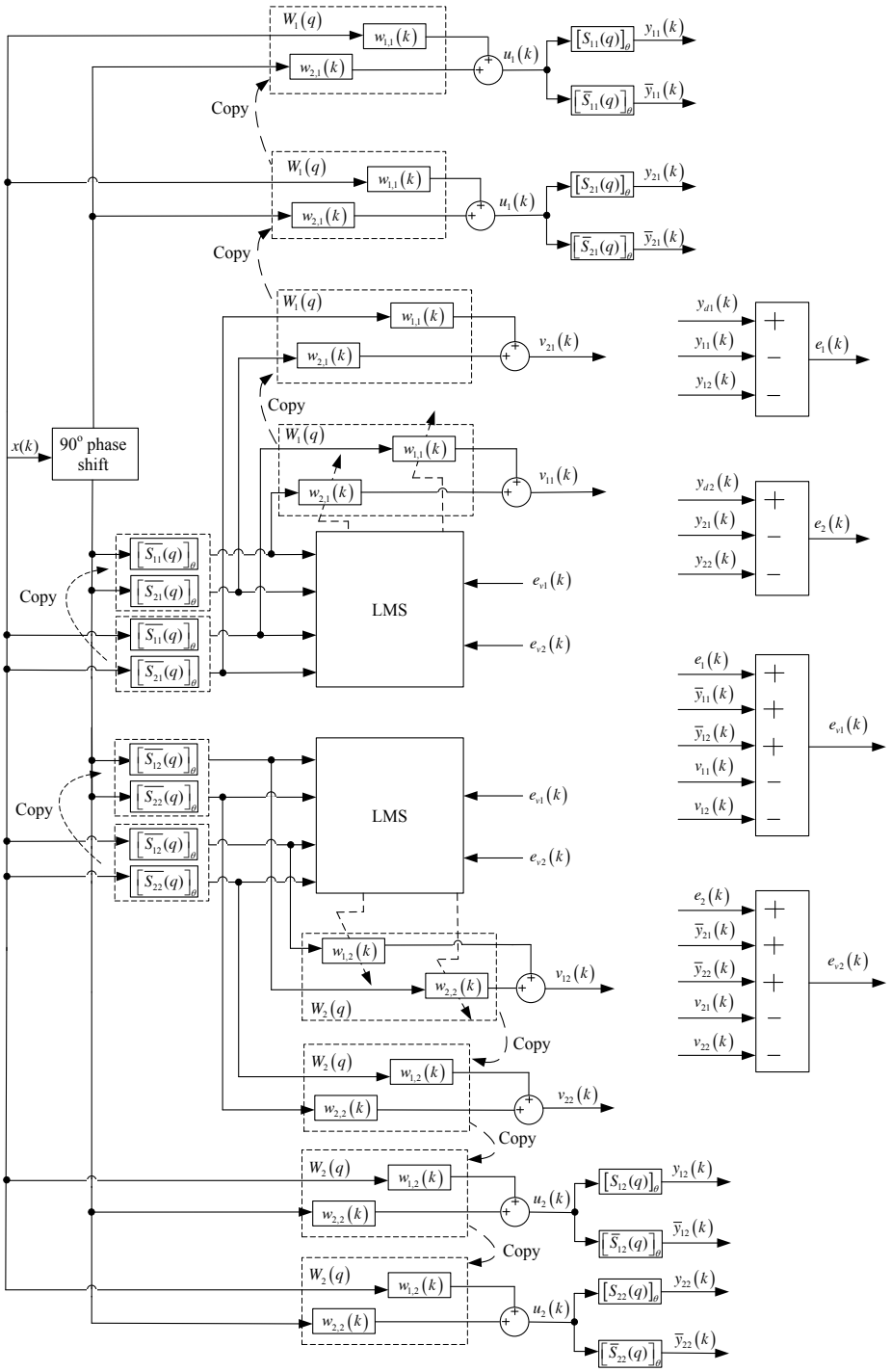

Figure 5. The flowchart of the MIMO form of the modified FxLMS control algorithm

4. EXPERIMENTAL VALIDATION

The purpose of the experiments in this section is to examine the performance of actively controlled PBRIAs in the test bed presented in the section 2. Prior to describing the results obtained, some system parameters are defined first. During the experimental study, the measured signals are recorded by a dSpace DS 2004 A/D acquiring board at a sampling frequency of 2.5 kHz. All the signals fed into the control board are filtered by a low pass filter with a 1k Hz cut-off frequency. The modified FxLMS controller is updated at a sampling frequency of 20 kHz. An encoder with a resolution of 1024 pulses per revolution is utilized to measure the rotational position of the shaft, the signals from which are then processed by the dSpace control broad 3001 to calculate the instant angular position. As described earlier, the horizontal acceleration of the plate and the vertical acceleration of the frame are taken as the error signals. The disturbance is provided by the electrodynamic shaker, which can execute dynamic forces on the shaft. The electrodynamic shaker is driven by a sinusoidal signal at 371 Hz throughout the study. This frequency corresponds to one of the resonances of the sound radiating plate. The whole control scheme is implemented in the Matlab Simulink environment and then downloaded to the processor of a dSpace 1006 system. The sine wave sent to the disturbance shaker is directly taken as the reference signal for the modified FxLMS controller in the Simulink model. In such a case, a perfect correlation between the reference and the disturbance is assumed. In real-life applications, a tacho signal, which provides information concerning the disturbance frequency, is always taken as the reference signal. This signal can be acquired for example from an optical sensor measuring the rotational motor speed. In order to assure an adequate level of coherence between the reference and disturbance signals, the measured pulse train can be fed into a frequency estimator to estimate the instant rotating speed [24].

The secondary plants are modelled by FIR filters, which can be estimated off-line with an LMS adaptive algorithm [2]. The process consists of exciting the secondary path with a sine wave and in the meanwhile providing the same signal as the reference to a conventional LMS algorithm. After the convergence of the algorithm, the controller coefficients will then resemble the secondary path impulse response. Since only a single frequency is considered, an FIR filter with only 2 coefficients is sufficient. By repeating this at multiple frequencies, the FIR filter coefficients for the secondary plants at all relevant frequencies can be inserted as a lookup table as a function of the disturbance frequency. An alternative is to measure the FRFs of the secondary paths in a broad frequency band, from which the FIR coefficients at one frequency can also be derived.

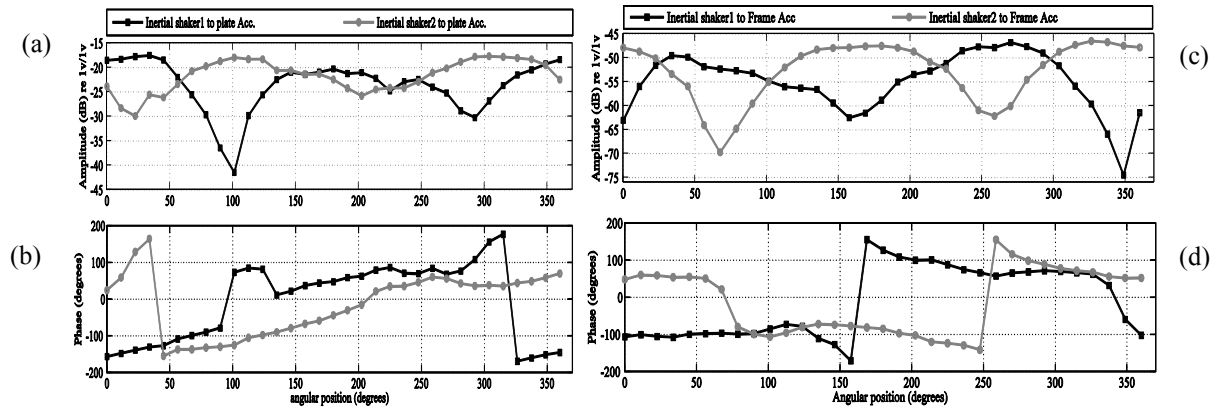

Figure 6. FRFs of the secondary plants at the 32 angular positions: (a) and (b), the amplitude and the phase of the FRFs between PBRIAs 1 and 2 to the horizontal plate vibration; (c) and (d), the amplitude and the phase of the FRFs between PBRIAs 1 and 2 to the vertical frame vibration.

As mentioned above, the constructed secondary plants are angular position dependent and an interpolation scheme is needed. Here, each secondary plant is identified at 32 angular positions in one revolution. The 0˚ position is defined when piezoelectric actuator of PBRIA 1, as shown in Figure 2, is in parallel to the disturbance. Figure 6 (a) and (b) show the amplitude and phase of the secondary-plant FRFs between the voltages to the piezoelectric actuators and the measured plate vibrations at 371 Hz, while Figure 6 (c) and (d) present the FRFs of the other two secondary-plants between the voltages to the piezoelectric actuators and the measured vertical frame vibrations. As can be seen, the four plants vary with respect to the angular positions, where the crests and troughs of the curves are located at these positions when the actuation direction of the PBRIA is parallel and perpendicular to the direction of the sensors.

Experiments with the proposed PBRIAs are performed when the shaft is rotating at 60, 120 and 180 rpm respectively. The aim here is to investigate the influence of the rotating speed to the proposed control approach. The convergence rate μ is set to 0.7 and the leaky factor β is set to 0.995. Here, certain power constraint is introduced, which is essential for the current MIMO control case where the plant matrix is nearly ill-conditioned. By doing it, unreasonable values of control effort are prevented. An additional benefit is to reduce the risk of instability and speed up the convergence of the insignificant errors 2.

Figure 7 (a) shows the measured plate vibrations at the rotating speed of 60 rpm, 120 rpm and 180 rpm (from top to bottom), first with the developed controller deactivated, then activated and again deactivated. It can be seen that the residue level drastically increases with an increase of the rotating speed, which indicates that the control effectiveness might further degrade as the shaft operates faster. In order to further analyze these results, the achieved reductions are plotted as a function of the rotational position of the shaft. To do so, the time domain signals of the first two segments (deactivated and activated) are synchronized with the rotating speed signal measured by the encoder, and the reductions are calculated in an interval of 10˚. The resultant reductions are shown in the angular domain in Figure 7 (b), where the average reductions during the different revolutions are represented by the dot-line and the variations by the error bars. As it is shown, the trend of the averaged reductions also shows the performance loss increases as the rotating speed increases.

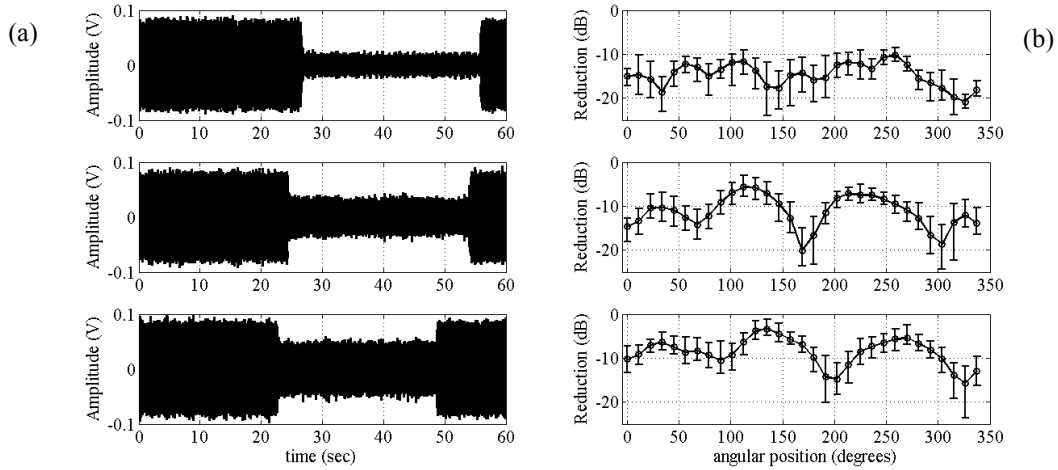

Figure 7: (a) The control effect on the plate vibrations when the shaft rotates at, from top to bottom, 60 rpm, 120 rpm and 180 rpm in the time domain; (b) The resultant reductions in the angular domain.

Next, the first two segments of the time domain signals in each case are projected into the frequency domain, as shown in Figure 8 (a). The achieved reductions are presented in Figure 8 (b), evaluated at the disturbance frequency itself and three pairs of rotating speed harmonics away from it. Here also, the achieved reductions at the excitation frequency reduce as the speed goes up. The main reason for the loss of the performance is that the faster change on the secondary plants makes it more challenging for the controller to follow and adapt to these changes but gets less and less time to do so. Additionally, the non-perfect estimation of the secondary plants and their nonlinearities, which means the secondary plants might vary in terms of the rotating speed, also contribute to the control effectiveness loss.

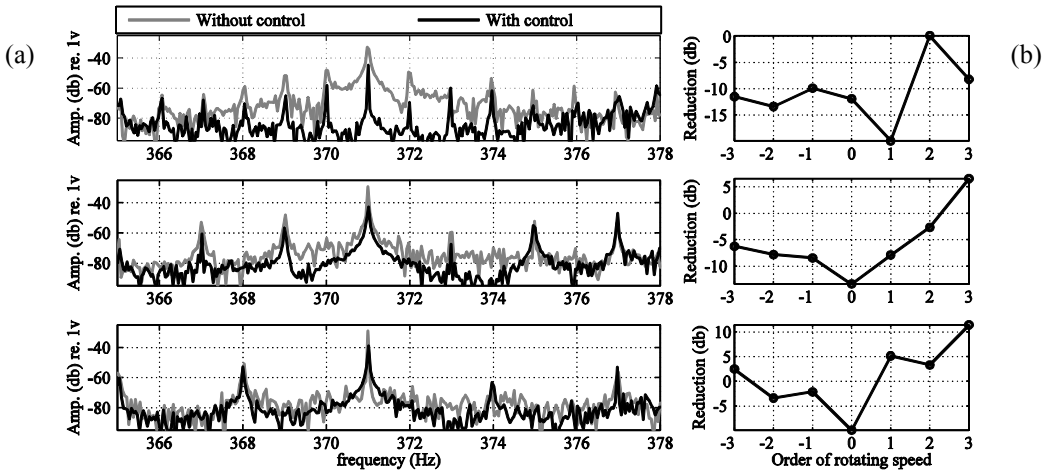

Figure 8: (a) Comparison of the plate vibrations in the frequency domain, without control and with control when the shaft rotates at, from top to bottom, 60 rpm, 120 rpm and 180 rpm; (b) the resultant reductions at the exciting frequency itself and three pairs of the rotating speed harmonics away from it.

The performance for the vertical frame vibrations is also examined, as shown Figure 9 and Figure 10. Compared to the plate vibrations, the control effectiveness has now completely disappeared and amplifications are even observed at higher rotating speed. This is mainly because the convergence speed of the vertical frame vibration is much less than the one of the plate vibration such that the initial transient of the coefficients are mainly determined by the plate vibration. With the increase of the rotating speed, the performance loss on the plate vibrations, as shown in Figure 7 and Figure 8, thus leads to the poor control effectiveness on the vertical frame vibrations. Since the emphasis in the study is on the plate vibrations, the behavior of the vertical frame acceleration is to be expected. Nevertheless, the proposed active controlled PBRIAs can work effectively in a low running speed condition.

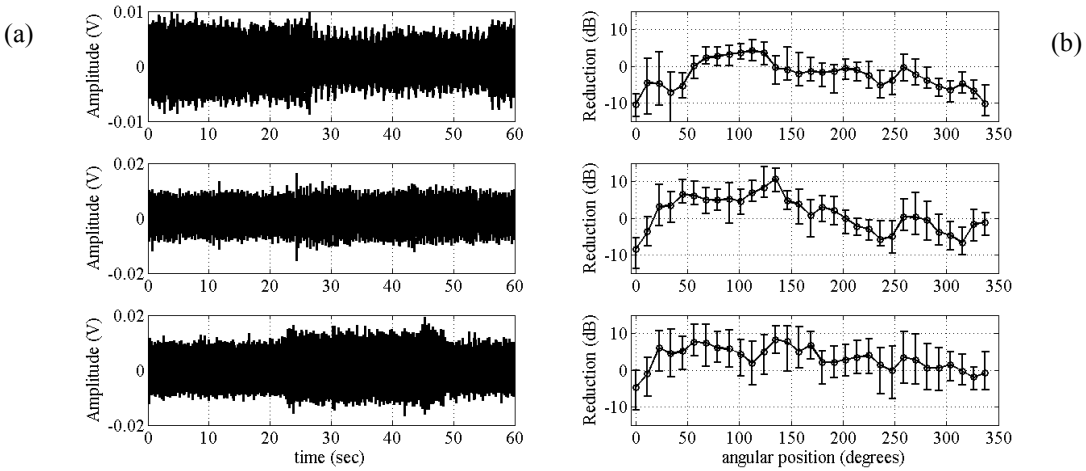

Figure 9: (a) The control effect on the vertical frame vibrations when the shaft rotates at 60 rpm, 120 rpm and 180 rpm in the time domain; (b) The resultant reductions in the angular domain.

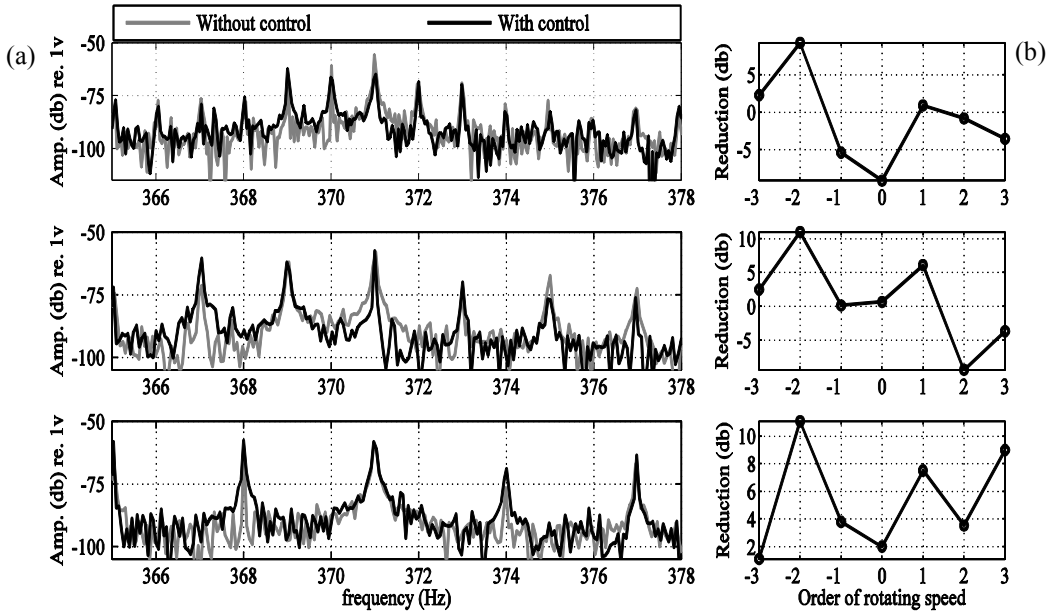

Figure 10: (a) Comparison of the vertical frame vibrations in the frequency domain, without control and with control when the shaft rotates at, from top to bottom, 60 rpm, 120 rpm and 180 rpm; (b) the resultant reductions at the exciting frequency itself and three pairs of the rotating speed harmonics away from it.

5. CONCLUSION

This paper discusses a novel control concept for suppressing rotating machinery radiating noise, which is to use PBRIAs that rotate together with the machinery to actively control the effects of disturbance forces transmitted to the structure housing. A MIMO form of the modified FxLMS algorithm is applied to control the plate vibrations and the frame vibrations. In order to account for the time varying effects of the rotating PBRIAs, a linear interpolation scheme is proposed to model the time varying secondary plants. The design and control approach have been validated on an experimental test bed. It has been shown that more than 7 dB reductions in the plate vibrations can be achieved when the shaft rotates below 180 rpm, with the resulting reduction of acoustic noise in the same order of magnitude. These results demonstrate the technical feasibility of using the considered PBRIAs for suppressing structure borne noise of rotating machinery for applications with a low running speed. Once the speeds become high however, the controller can have difficulties following and adapting fast enough. Additionally, the non-perfect estimation of the secondary plants and their nonlinearities are more pronounced. Therefore, future studies will aim at improving the performance of the active vibration control approach for higher rotating speeds, as well as gaining a better understanding of the limitations of the followed approach.

ACKNOWLEDGMENTS

The IWT Flanders within the OptiWind project (GA: IWT/120029), the Research Fund KU Leuven and the European Commission within the ITN EMVeM Marie Curie project (GA: 315967) are gratefully acknowledged for their support to Guoying Zhao. The China Scholarship Council is also gratefully acknowledged. The research performed by Neven Alujević was supported financially through an EU FP7 Marie Curie Industry-Academia Partnerships and Pathways (IAPP) Grant Agreement 251211.

REFERENCES

1. P.A. Nelson, S.J. Elliott, Active control of Sound, *Academic Press*, New York, 1992
2. S.M. Kuo, D.R. Morgan, Active Noise Control Systems: Algorithms and DSP Implementation, *Wiley*, New York, 1996.
3. S.J. Elliott, C.C. Boucher and P.A. Nelson, The behaviour of a multiple channel active control system, *IEEE transactions on Signal Processing* (1992), Vol. 40(5), 1041-1052.
4. S. J. Elliott, P. A. Nelson, I. M. Stothers. And C. C. Boucher, Inflight experiments on the active control of propeller-induced cabin noise, *Journal of Sound and Vibration*, vol. 140. pp. 219-238, 1990.
5. W. Dehandschutter, The reduction of structure-borne noise by active control of vibration, PhD thesis, *KU Leuven*, Leuven, Belgium (1997).
6. G. Pinte**,** Active Control of Repetitive Impact Noise, PhD thesis, *KU Leuven*, Leuven, Belgium. (2007).
7. Den Hartog, J. P., Mechanical Vibrations, *McGraw-Hill Book Co*., New York, (1934.)
8. J. B. Hunt**,** Dynamic Vibration Absorbers**,** London: *Mechanical Engineering Publications Ltd*. (1979).
9. D. J. Inman, Engineering Vibration, *Prentice-Hall*, New York (1994).
10. N. Alujevic, I. Tomac and P. Gardonio, Tunable vibration absorber using acceleration and displacement feedback, *Journal of Sound and Vibration* (2012) 331(12), 2713-2728.
11. C. Paulitsch, P. Gardonio, S. J. Elliott, P. Sas, and R. Boonen, Design of a Lightweight, Electrodynamic, Inertial Actuator with Integrated Velocity Sensor for Active Vibration Control of a Thin Lightly-Damped Panel, *International Conference on Noise and Vibration Engineering (ISMA)*, KU Leuven, Belgium, 20-23 September 2004.
12. C. Paulitsch, P. Gardonio, S.J. Elliott, Active vibration control using an inertial actuator with internal damping, *Journal of the Acoustical Society of America* 119 (2006) 2131–2140.
13. N. Alujevic, G. Zhao, B. Depraetere, P. Sas, B. Pluymers and W. Desmet, $\mathcal{H}_2$ optimal vibration control using inertial actuators and a comparison with tuned mass dampers, *Journal of Sound and Vibration* (2014), 333(18), 4073-4083.
14. N. Alujevic, P. Gardonio, and K. D. Frampton, Smart double panel for the sound radiation control: blended velocity feedback. *AIAA Journal*, vol. 49. No. 6 (2011), pp. 1123-1134.
15. Z. Qiu, X. Zhang, H. Wu and H. Zhang, Optimal placement and active vibration control for piezoelectric smart flexible cantilever plate, *Journal of Sound and Vibration* (2007) 301, 521-543.
16. E. Crawley and J. de Luis, Use of piezoelectric actuators as elements of intelligent structures, *AIAA Journal* 25 (1987) 1373-1385.
17. C. R. Fuller, S. J. Elliott and P. A. Nelson, Active control of Vibration, *Academic Press*, San Diego, CA92101, 1986.
18. T. J. Sutton, S. J. Elliott, M. J. Brennan, K. H. Heron and D. A. C. Jessop, Active Isolation of Multiple Structural Waves on a Helicopter Gearbox Support Strut, *Journal of Sound and Vibration* (1997) 205(1), 81-101.
19. B. Rebbechi, C. Howard and C. Hansen, Active control of gearbox vibration, *Proceedings of the Active control of Sound*, Vibration conference, Fort Lauderdale, 1999, pp. 295-304.
20. G. Pinte, S. Devos, B. Stallaert, W. Symens, J. Swevers and P. Sas, A piezo-based bearing for the active structural acoustic control of rotating machinery. *Journal of Sound and Vibration*, 329 (2010) 1235-1253.
21. B. Stallaert, Active structural acoustic source control of rotating machinery, PhD thesis, *KU Leuven* (2010).

22. M. H. Chen, M. J. Brennan, Active control of gear vibration using specially configured sensors and actuators, *Smart Materials and Structures* 9(3) 2000 342-350.
23. Y.H. Guan, M. Li, T.C. Lim and W.S. Shenpard Jr., Comparative analysis of actuator concepts for active gear pair vibration control, *Journal of Sound and Vibration*, 269 (1-2) (2004) 273-294.
24. Y.H. Guan, T.C. Lim and W.S. Shenpard Jr., Experimental study on active vibration control of a gearbox system, *Journal of Sound and Vibration*, 282 (3-5) (2005) 713-733.
25. M. Li, T.C. Lim, W.S. Shenpard Jr. Y.H. Guan, Experimental active vibration control of gear mesh harmonics in a power recirculation gearbox system using a piezoelectric stack actuator, *Smart Materials and Structures*, 14 (5) (2005) 917-927.
26. C. Bao, Adaptive algorithms for active noise control and their applications, PhD thesis, *KU Leuven*, Leuven, Belgium. (2007).
27. C. Bao, P. Sas and H. van Brussel, A novel filtered-x lms algorithm and its application to active noise control, *In: Signal Processing VI - Theories and Applications*.Proceedings of EUSIPCO-92, Sixth European Signal Processing Conference 3(1992), pp. 1709–1712.
28. S.M. Kuo and D.R. Morgan, Active noise control: a tutorial review, *Proceedings of the IEEE* (1999), Vol. 87(6), 943-973.